Journal of Magnetic Resonance **150,** 178–183 (2001)
doi:10.1006/jmre.2001.2339, available online at http://www.idealibrary.com on IDEAL®

Effects of Higher Rank Multipoles on Relaxation of an $I = 3$ Spin System

W. Nosel,* S. Capuani,† D. Capitani,‡ and F. De Luca†,[1]

*Marian Smoluchowski Institute of Physics, Jagiellonian University, Reymonta 4, 30-059 Kracow, Poland; †Physics Department and INFM, University of Rome "La Sapienza," I-00185 Rome, Italy; and ‡Institute of Nuclear Chemistry, CNR Research Area, I-00100 Montelibretti, Italy

Received November 22, 2000; revised January 29, 2001

Magnetic multipoles of rank higher than one become active in spin systems with $I > 1/2$ and their contribution to relaxation depends on dynamics. The appearance of multipole terms complicates the relaxation description and supports the multiexponential behavior of relaxation. In this paper the effects of high-rank multipoles on lineshape and longitudinal relaxation of $I = 3$ spin systems are presented. Results obtained from both numerical simulation and experimental data show that longitudinal and transverse relaxation are strongly influenced by these multipole terms, especially at lower temperature where, due to lower molecular mobility, the extreme narrowing condition is not fulfilled.

Key Words: **^{10}B-NMR; higher rank multipoles.**

INTRODUCTION

Nowadays it is widely recognized that NMR relaxation is a powerful tool for studying the dynamics of macromolecular aggregates (*1*, *2*). It is also a common belief that such aggregates are characterized by "slow" motion, which often conveys relaxation outside the extreme narrowing regime and produces differences in the spectral densities involved. In such a case, for spins $I > 1/2$, the NMR relaxation can no longer be described by a single exponential because, in addition to the frequency dependence (*3*, *4*), state multipoles of rank higher than one (*5*) contribute to the relaxation process. This latter aspect, not yet fully recognized, could influence, for example, the relaxation data obtained from inversion recovery experiments (*6*–*8*) by complicating their interpretation, especially for higher spin quantum numbers.

It has been shown that in an isotropic molecular system the decay of magnetization is described by $I + 1/2$ exponential functions for half integer spins and by I exponential for integer ones (*9*). While the case of $I = 3/2$ has been explicitly solved (*9*, *10*), the cases of $I = 5/2$ and $I = 7/2$ have been dialed with the aid of numerical approximations (*11*). In spin systems with $I = 3/2$, $5/2$, and $7/2$, it has also been demonstrated that the effect of higher rank multipoles depends on the pulse sequence parameters and on the thermodynamic state of magnetization (*6*). For example, when spectra are recorded using the residual magnetization available near the inversion recovery null-point condition, the effect of higher rank multipole terms is particularly significant (*7*, *8*).

Because of the great importance of the ^{10}B nuclei in biology and biomedicine (*12*) and also for the sake of completeness, to include integer spins, we extended the analysis to the $I = 3$ spin. The theory of relaxation of the so-called "states of multipoles" (*13*) is based on Redfield's semiclassical theory of relaxation (*14*).

The experiments on ^{10}B have been realized on samples of $Na_2{}^{10}B_{12}H_{11}SH$ (BSH), a molecular compound where each ^{10}B nucleus is bound to four other ^{10}B and by covalent link to one hydrogen nucleus. The BSH, currently the most promising molecule for BNCT (boron neutron capture therapy (*15*)), has been studied using glycerin as a solvent so that the condition of a nonextreme narrowing regime is better fulfilled at different temperatures. To prove that the thermodynamic state of magnetization influences the appearance of effects related to higher rank multipoles, the lineshape has also been measured by inversion recovery experiments under conditions where the magnetization was prepared to be more or less close the thermodynamic equilibrium. The inversion recovery experiments, performed at different temperatures, show that the longitudinal relaxation is well described by a multiexponential decay as predicted by multipoles theory while the lineshapes behave as those of half integer quadrupolar nuclei. In addition, the influence of dynamics on the multipoles effect has been fully confirmed.

THEORY

Following Einarsson and Westlund (*6*), we describe the relaxation of $I = 3$ nuclei by means of a spin system density matrix (*12*) within the framework of the Bloch–Wangsness–Redfield relaxation theory (*14*, *16*, *17*). The relaxation of longitudinal components of state multipoles σ_0^K (*18*, *19*) is therefore described by

$$\frac{d}{dt}\sigma_0^K(t) = \sum_{K'} R_{00}^{KK'}\left(\sigma_0^{K'}(t) - \sigma_{0\,\mathrm{eq}}^{K'}\right), \qquad [1]$$

where

$$\sigma_m^K = \sum_\alpha \rho_{\alpha\alpha}(-1)^{I-\alpha}(2K+1)^{1/2}\begin{pmatrix} I & I & K \\ \alpha & -\alpha & m \end{pmatrix} \qquad [2]$$

[1] To whom correspondence should be addressed.

1090-7807/01 $35.00

and K denotes the rank of state multipoles here expressed by Wigner 3-j symbols (*18*). The subscript eq denotes the thermodynamic equilibrium condition and $\rho_{\alpha\alpha}$ are the density matrix elements in representation $\{|\alpha\rangle\}$ that diagonalizes the static Hamiltonian; $R_{00}^{KK'}$ indicate the elements of the relaxation supermatrix for state multipoles given by (*18, 20, 21*)

$$R_{00}^{KK'} = \sum_{\alpha\beta} R_{\alpha\alpha\beta\beta}(-1)^{2I-\alpha-\beta}(2K+1)^{1/2}(2K'+1)^{1/2} \times \begin{pmatrix} I & I & K \\ \alpha & -\alpha & 0 \end{pmatrix} \begin{pmatrix} I & I & K' \\ \beta & -\beta & 0 \end{pmatrix}. \quad [3]$$

For $I = 3$ there exist $2I$ multipoles with $K = 1, 2, \ldots, 6$ (dipole, quadrupole, octupole, 16-pole, 32-pole, and 64-pole). However, because quadrupolar relaxation couples only even or only odd rank of state multipoles, the dipole, octupole, and 32-pole evolutions are governed by the system of three coupled first-order differential equations, which for

$$X_0^K(t) = \sigma_0^K(t) - \sigma_{0\,\mathrm{eq}}^K \quad [4]$$

has the form

$$\frac{d}{dt}X_0^K(t) = \sum_{K'=1,3,5} R_{00}^{KK'} X_0^{K'}(t). \quad [5]$$

For this system the initial conditions, after a π pulse, in high temperature approximation, are given by $X_m^K(0) = -\frac{4\omega_0}{\sqrt{7}kT}\delta_{K1}\delta_{m0}$. The $R_{00}^{KK'}$ matrix elements are reported in Table 1 where only terms with $|K - K'| = 0, 2$ have been taken into account (*6*). The elements of the relaxation matrix have been evaluated for quadrupolar interaction with vanishing time-average values.

The solution of system [5] may be presented in the form

$$X_0^K(t) = C_K \sum_{i=1,2,3} A_i^K e^{S_i t}, \quad [6]$$

where $C_1 = C_5 = X_0^1(0)$ and $C_3 = -C_1$. In other words, the relaxation of each state multipole is described by a linear combination of three exponential functions characterized by different A_i^K amplitudes and different S_i relaxation rate exponents. The explicit forms of the A_i^K amplitudes and of the S_i exponents are calculated in the Appendix.

TABLE 1
$R_{00}^{KK'}$ Matrix Elements for $I = 3$ spins

$R_{00}^{11} = -\frac{27}{20}A_Q^2(j(\omega_0) + 4j(2\omega_0))$
$R_{00}^{13} = R_{00}^{31} = -\frac{108}{5\sqrt{42}}A_Q^2(j(\omega_0) - j(2\omega_0))$
$R_{00}^{33} = -\frac{3}{10}A_Q^2(51j(\omega_0) + 54j(2\omega_0))$
$R_{00}^{35} = R_{00}^{53} = -\frac{36}{\sqrt{14}}A_Q^2(j(\omega_0) - j(2\omega_0))$
$R_{00}^{55} = -\frac{9}{4}A_Q^2(9j(\omega_0) + 8j(2\omega_0))$

Note. A_Q is the quadrupolar coupling constant.

The numerical analysis of results shows that for $K = 1$ two of the three amplitudes A_i^1's are negligible while for multipoles of rank $K = 3$ and $K = 5$ all of the amplitudes A_1^K, A_2^K, and A_3^K are notable and their values decrease to zero upon increasing the rate of molecular motion τ_c^{-1} (Fig. 1).

In Fig. 2 the simulated time evolution of the longitudinal components of dipole, octupole, and 32-pole is presented for an inversion recovery experiment as in Eq. [6]. The results show that the multipoles of rank 3 and 5 reach their maximum values at about the null-point time, in agreement with the results obtained on half integer spins (*6, 22*). In Fig. 3 the time evolution of longitudinal components of dipole, octupole, and 32-pole is simulated as functions of the correlation time τ_c. The plots show that the amplitudes and the time positions of the octupole and of the 32-pole maxima depend on $\omega_0\tau_c$: for higher $\omega_0\tau_c$, that is very far away from the extreme narrowing condition, the maxima with higher amplitudes are located around the null-point time site. On the other hand, in the extreme narrowing limit, the ranks of multipoles are conserved during relaxation and the longitudinal component of magnetization, which is determined by σ_0^1, relaxes exponentially with rate R_{00}^{11}. The results of Figs. 2 and 3 have been obtained with $\omega_0 \cong 64$ MHz (the resonance frequency of ^{10}B in a magnetic field of 600 MHz for proton) and $A_Q = 1.25$ MHz, the quadrupolar coupling constant of ^{10}B nuclei in BSH (*23*).

EXPERIMENTAL RESULTS AND DISCUSSION

All measurements were performed on a Bruker AMX 600 spectrometer. The ^{10}B spin–lattice relaxation and the ^{10}B lineshapes, measured on the magnetization close the null-point time, were obtained on a sample composed by 95% ^{10}B-enriched BSH (purchased from Boron Biologicals) and glycerin to slow down the BSH dynamics even at room temperature. The ^{10}B spectrum of BSH dissolved in D_2O at $\omega_0 \cong 64$ MHz is reported in Fig. 4.

T_1 experiments were performed using a standard inversion recovery pulse sequence with about 40 time points for each measurement. The 180° pulses duration were from about 20 to about 30 μs depending on temperature. In Table 2 the ^{10}B longitudinal relaxation times measured at six temperatures ranging from 238 to 300 K are reported as calculated using multiexponential fitting functions. The best results have been obtained by a three-exponential fit at $T = 238$ K and $T = 243$ K, by a two-exponential decay at $T = 248$ K, 258 K, and 278 K, and by a monoexponential decay at $T = 300$ K, according to the provisions of Fig. 3. The effect of higher multipoles on relaxation becomes less effective as molecular mobility increases. In this case the octupole term is much greater than the 32-pole term but both are much smaller than dipole: thus just octupole appreciably affects the dipolar line.

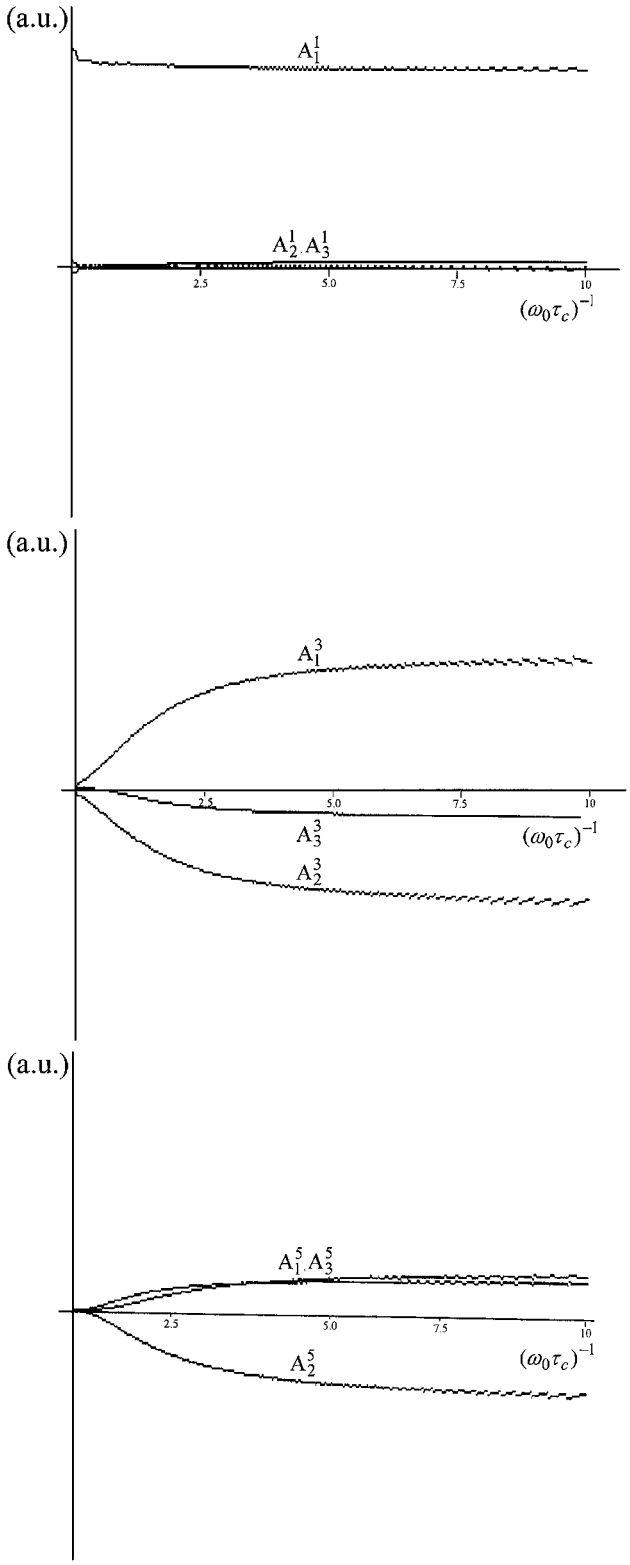

FIG. 1. The amplitudes A_i^K which characterize the relaxation of each state multipole described by the linear combinations, Eq. [A8]. For $K=1$, the numerical calculation shows that A_2^1 and A_3^1 are in practice negligible. The amplitudes of $K=3$ (octupole) and $K=5$ (32-pole) are roughly equivalent and decrease as the rate of molecular motion τ_c^{-1} increases.

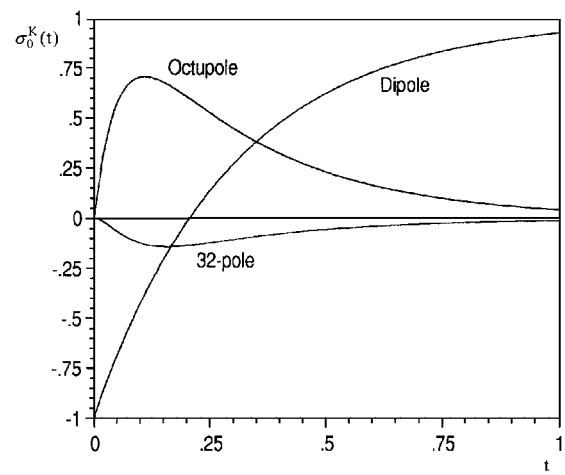

FIG. 2. Time evolution of the longitudinal components of state multipoles σ_0^K (for dipole, octupole, and 32-pole) during the delay t between the inversion recovery pulses. The simulation has been performed for $\omega_0\tau_c = 1$, where $\omega_0 =$ 64 MHz and $A_Q = 1.25$ MHz.

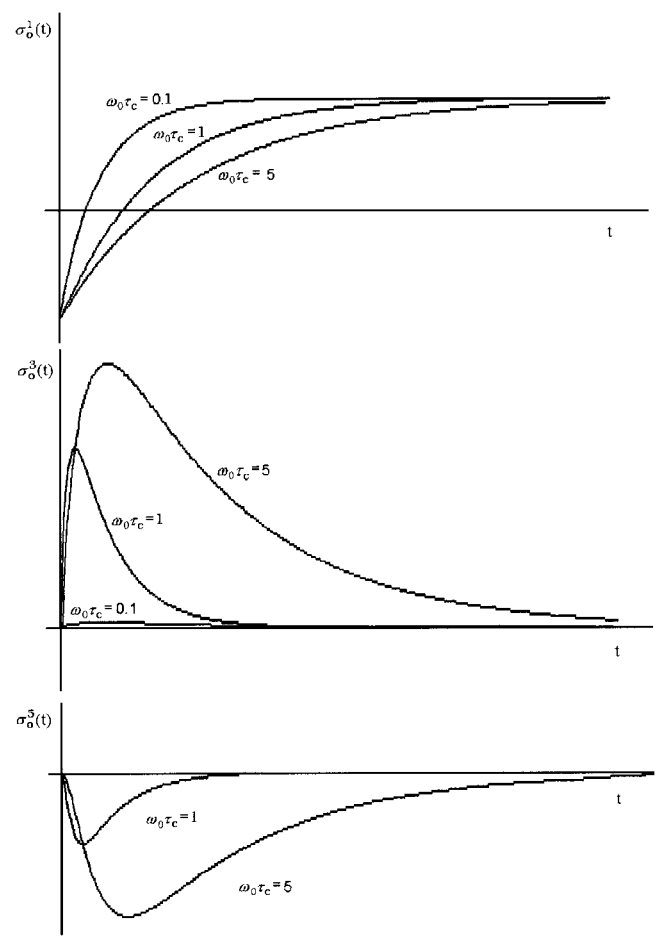

FIG. 3. Plots of the σ_0^1 (dipole), σ_0^3 (octupole), and σ_0^5 (32-pole) time evolution during the delay t between the π and the $\pi/2$ pulses of the inversion recovery sequence by varying $\omega_0\tau_c$. The simulation has been realized by using $\omega_0 = 64$ MHz and $A_Q = 1.25$ MHz.

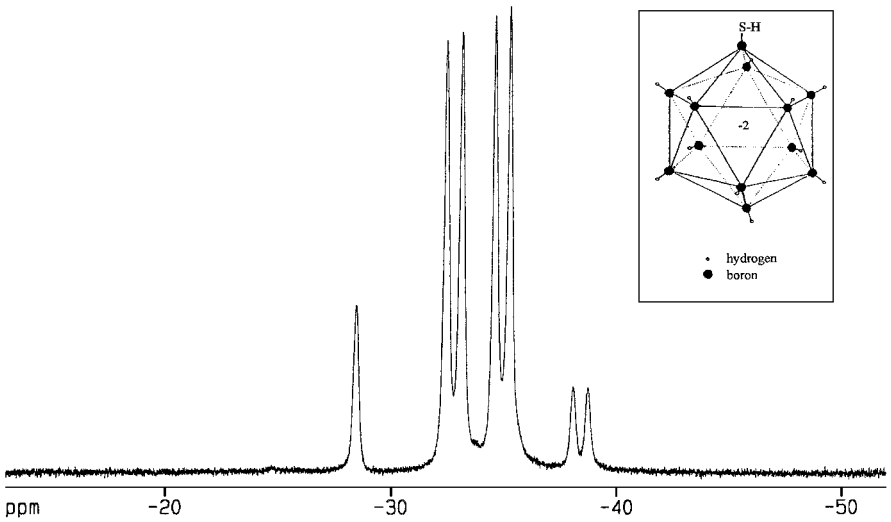

FIG. 4. ^{10}B spectrum at $\omega_0 = 64$ MHz of 75 mM of ^{10}B 95%-enriched BSH in D_2O at 300 K. The structure of the molecule in solution (BSH anion) is reported in the inset. In the molecule each boron atom is coupled to one hydrogen, except for one boron atom, which is bound to the sulfur of the SH group. The spectrum shows four resonances, which are associated to the four nonequivalent boron sites. Because of the J-coupling with protons, each line of the spectrum (except for that associated with sulfur) shows a doublet with spacing of about 41 Hz. The spectrum was acquired in a single scan and apodized with a 8-Hz line broadening function. The zero frequency corresponds to the resonance of the ^{10}B of boric acid.

In Figs. 5 and 6 the experimental ^{10}B lineshapes at different temperatures are shown. For each temperature, the lineshape obtained from magnetization near the null-point time and the lineshape obtained using a single 90° pulse, corresponding to equilibrium magnetization, are reported and compared. At temperatures of 238, 243, and 248 K (Figs. 5a, 5b, and 5c, respectively) the spectral lines obtained near the null-point are slightly narrower with respect to the ones obtained from equilibrium magnetization; the effect is more evident at the lowest temperature ($T = 238$ K), where the condition of extreme narrowing is least fulfilled. On the other hand, at temperatures of 258, 278, and 300 K (Figs. 6a, 6b, and 6c, respectively) the spectral lines obtained in inversion recovery experiments are slightly larger than those obtained from equilibrium magnetization. Furthermore, at 278 K, the spectrum of inversion recovery experiment shows two peaks, while the corresponding equilibrium lineshape does not exhibit structure. A similar situation is also present at

TABLE 2
The ^{10}B Longitudinal Relaxation Times, Measured at Six Temperatures, Are Reported

T	T_1^{I}	T_1^{II}	T_1^{III}
238 K	7.00 ± 0.1 (80)	10.00 ± 0.2 (8)	17.6 ± 0.4 (12)
243 K	1.3 ± 0.1 (70)	8.7 ± 0.2 (18)	14.7 ± 0.4 (12)
248 K	4.23 ± 0.04 (78)	8.1 ± 0.3 (10)	11.0 ± 0.4 (12)
258 K	1.10 ± 0.05 (85)	3.5 ± 0.1 (15)	
278 K	1.25 ± 0.05 (96)	1.46 ± 0.05 (4)	
300 K	4.07 ± 0.04 (100)		

Note. The relative amplitudes of the various relaxation components $T_1^{\mathrm{I,II,III}}$ are reported in parentheses as a percentage.

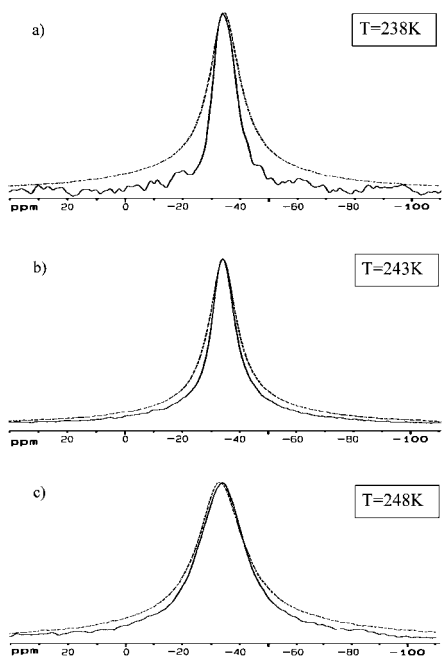

FIG. 5. Experimental ^{10}B lineshapes at $T = 238$ K (a), 243 K (b), and 248 K (c). The linewidths of spectra obtained from magnetization detected near the null-point time in the inversion recovery experiment (solid line) are narrowed with respect to lineshapes obtained from equilibrium magnetization (dashed line). This effect is "amplified" at lower temperature. The inversion recovery spectra were obtained by averaging 64 scans, each taken with a recycling time of 1 s and delays between the inversion recovery pulses of $t = 4$ ms ($T = 238$ K), $t = 3$ ms ($T = 243$ K), and $t = 2.5$ ms ($T = 248$ K); spectra from equilibrium magnetization were acquired after a single $\pi/2$ pulse by averaging 8 scans with 1 s of recycling delay. Also in this case the zero frequency refers to the resonance of ^{10}B of boric acid.

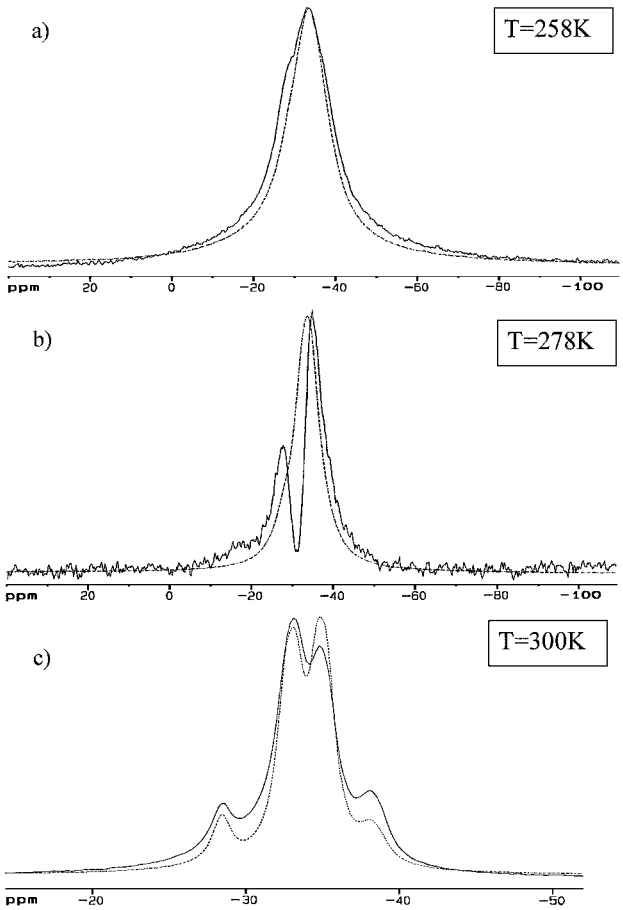

FIG. 6. Experimental ^{10}B lineshapes at $T = 258$ K (a), 278 K (b), and 300 K (c). The linewidths of spectra obtained near the null-point (solid line) are slightly broadened with respect to the lineshapes obtained at equilibrium (dashed line). The inversion recovery spectra were obtained by averaging 64 scans with a recycling delay of 1 s and with $t = 1$ ms ($T = 258$ K), $t = 0.8$ ms ($T = 278$ K), and $t = 3$ ms ($T = 300$ K). The spectra from equilibrium magnetization were obtained as were those in Fig. 5.

$T = 258$ K, to a lesser extent. Thus, in general, the comparison of lineshapes obtained from magnetization detected near the null-point time with the ones obtained from equilibrium magnetization is in agreement with that reported for half integer spins (*6*).

However, since the $I = 3$ spins are part of the BSH molecule, the ^{10}B lineshapes should show some structure related to the magnetic site symmetry of molecule. In Fig. 6c, for example, each of the two spectra is made up of four lines due to the four nonequivalent boron sites of the BSH molecule (see also Fig. 4). The spectrum shows an evident asymmetry of the two inner lines compared with that obtained from equilibrium magnetization. This can be reasonably explained as a consequence of the dynamics shift (*18*), which is responsible for nonsymmetric signal and which makes the phase adjustment a difficult problem.

This appears to be the first time that the effects of higher rank multipoles have been evaluated on $I = 3$ nuclei. The experimental data have been obtained on ^{10}B of BSH molecules in glycerin, at different temperatures, by an inversion recovery pulse sequence and a simple 90° pulse excitation. The experimental data are in agreement with the theory developed on a similar basis of that already existing for half integer quadrupolar nuclei.

This contribution can be seen as an extension of the higher rank multipole theory and it may be able to furnish important information to perform quantitative ^{10}B spectroscopy of boron compounds as it is needed, for example, to optimize BNCT.

The relaxation related to higher rank multipoles can be used as an extension or as a complementary tool to the traditional relaxation experiments to study biological systems in order to characterize in detail their dynamics, especially their slower dynamics.

APPENDIX

The Laplace transformation of the system Eq. [5],

$$\frac{d}{dt}X_0^K(t) = \sum_{K'=1,3,5} R_{00}^{KK'} X_0^{K'}(t), \qquad [A1]$$

leads to an inhomogeneous system of algebraic equations whose solution may be expressed in the form

$$X_0^K(S) = \frac{\sum_{K'=1,3,5} X_0^{K'}(t_1) D_{KK'}(S)}{D(S)}, \qquad [A2]$$

where $D_{KK'}(S)$ are algebraic complements of the corresponding matrix and

$$D(S) = \det\left(R_{00}^{KK'} - S\delta_{KK'}\right) = \prod_{i=1}^{3}(S - S_i). \qquad [A3]$$

The roots S_I of the characteristic equations have the form

$$\begin{aligned} S_1 &= 2\sqrt{\frac{-p}{3}}\cos\frac{\varphi}{3} - \frac{a_1}{3} \\ S_{2,3} &= -2\sqrt{\frac{-p}{3}}\cos\left(\frac{\varphi}{3} \pm \frac{\pi}{3}\right) - \frac{a_1}{3}, \end{aligned} \qquad [A4]$$

where

$$p = a_2 - \frac{a_1^2}{3}, \quad q = \frac{2}{27}a_1^3 - \frac{a_1 a_2}{3}, \quad \cos\varphi = \frac{-q}{2\sqrt{-\frac{p^3}{27}}} \qquad [A5]$$

and

$$\begin{aligned} a_1 &= -R_{00}^{11} - R_{00}^{33} - R_{00}^{55} \\ a_2 &= -\left(R_{00}^{13}\right)^2 - \left(R_{00}^{35}\right)^2 + R_{00}^{11}R_{00}^{33} + R_{00}^{11}R_{00}^{55} + R_{00}^{33}R_{00}^{55} \\ a_3 &= -R_{00}^{11}R_{00}^{33}R_{00}^{55} + R_{00}^{55}\left(R_{00}^{35}\right)^2 + R_{00}^{11}\left(R_{00}^{35}\right)^2. \end{aligned} \qquad [A6]$$

The solution of the system [A1] satisfies the initial conditions $X_m^K(0) = -\frac{4\omega_0}{\sqrt{7}kT}\delta_{Kl}\delta_{m0}$ and may be written in the form

$$X_0^K(t) = C_K \sum_{i=1,2,3} A_i^K e^{S_i t}, \qquad [A7]$$

where (see also Table 1)

$$A_i^1 = \frac{S_i^2 - \left(R_{00}^{55} + R_{00}^{33}\right)S_i + R_{00}^{33}R_{00}^{55} - \left(R_{00}^{35}\right)^2}{\prod_{k\neq i}(S_k - S_i)}$$

$$A_i^3 = \frac{\left(R_{00}^{55} - S_i\right)R_{00}^{13}}{\prod_{k\neq i}(S_k - S_i)} \qquad [A8]$$

$$A_i^5 = \frac{R_{00}^{13}R_{00}^{35}}{\prod_{k\neq i}(S_k - S_i)}$$

are the amplitudes associated to the longitudinal recovery of dipole (A_i^1), octupole (A_i^3), and 32-pole (A_i^5) state.

REFERENCES

1. A. D. McLachlan, *Proc. R. Soc. London Ser. A* **280,** 271 (1964).
2. A. Carrington and G. R. Luckhurst, *Mol. Phys.* **8,** 125 (1964).
3. T. E. Bull, *J. Magn. Reson.* **8,** 344 (1972).
4. T. E. Bull, S. Forsen, and D. L. Turner, *J. Chem. Phys.* **70,** 3106 (1979).
5. B. C. Sanctuary, T. K. Halstead, and P. A. Osment, *Mol. Phys.* **49,** 753 (1983).
6. L. Einarsson and P. O. Westlund, *J. Magn. Reson.* **79,** 54 (1988).
7. W. S. Price, N. H. Ge, and L. P. Hwang, *J. Magn. Reson.* **98,** 134 (1992).
8. W. T. Chang, Z. S. Shen, W. S. Price, N. H. Ge, and L. P. Hwang, *J. Magn. Reson. A* **109,** 98 (1994).
9. P. S. Hubbard, *J. Chem. Phys.* **53,** 985 (1970).
10. T. K. Halstead, P. A. Osment, B. C. Sanctuary, J. Tagenfeldt, and I. J. Lowe, *J. Magn. Reson.* **67,** 267 (1986).
11. J. Reuben and Z. Luz, *J. Phys. Chem.* **80,** 1357 (1976).
12. P. Bendel, *J. Magn. Reson. A* **117,** 143 (1995).
13. B. C. Sanctuary, *J. Magn. Reson.* **61,** 116 (1985).
14. R. K. Wangsness and F. Bloch, *Phys. Rev.* **89,** 728 (1953).
15. See, for example, Proceedings of the Seventh International Symposium on Neutron Capture Therapy for Cancer, Advanced in Neutron Capture Therapy, Vols. I and II, Zürich, Switzerland, 4–7 September, 1996 (B. Larsson, J. Crawford, and R. Weinreich, Ed.), Elsevier, 1997.
16. A. G. Redfield, *in* "Advances in Magnetic Resonance" (J. S. Waugh, Ed.), Vol. 1, p. 1, Academic Press, San Diego, 1965.
17. R. Hoffman, *in* "Advances in Magnetic Resonance" (J. S. Waugh, Ed.), Vol. 4, p. 87, Academic Press, New York, 1970.
18. P. O. Westlund and H. Wennerström, *J. Magn. Reson.* **50,** 451 (1982).
19. P. M. Brink and G. R. Satchler, "Angular Momentum," Oxford Univ. Press, London, 1968.
20. K. Blum, "Density Matrix Theory and Application," Plenum Press, New York, 1981.
21. B. C. Sanctuary and L. Selwyn, *J. Chem. Phys.* **74,** 906 (1981).
22. W. T. Chang, Z. S. Shen, W. S. Price, N. H. Ge, and L. P. Hwang, *J. Magn. Reson. A* **109,** 98 (1994).
23. A. Baram and P. Bendel, *J. Magn. Reson.* **129,** 10 (1997).